Vol. 37 No. 1 Transactions of Information Processing Society of Japan Jan. 1996

Regular Paper

Image Morphing by Spatial Thin-Plate Spline Transformation

RONGHUA YAN,† NAOYUKI TOKUDA,† JUICHI MIYAMICHI† and YONGMAO NI††

This paper presents a new morphing technique using a computationally efficient, globally valid spatial transformation method. The transformation employed is developed on a most general paradigm of a minimum norm of higher order derivatives of displacement squared, of which the thin-plate spline transformation of a minimum bending energy is the best known and is extensively used in deformation of 2D curves and 3D parametric curved surfaces. Compared with the other morphing techniques, the present algorithm is efficient not only in time complexity but also in reproducing descriptive, and yet smoothly interpolated morphed images with only a remarkably small number of feature points specified. The improved efficiency comes in part from the small number of feature points needed in the transformation thus requiring only a nominal time in matrix inversion and also from the block region based image reconstruction scheme used rather than a pixel by pixel based scheme where the image is reconstructed by linear interpolation within the block rather than going through summations over all feature points. We demonstrate that a considerable saving can be achieved in time complexity without sacrificing the quality of the image reconstructed. The method also has a capability of localizing distortions due to morphing, an important feature in animation applications by simply adding constraining feature points along a region of localization. We have applied the 2D version of the present transformation to a 2.5-D application of a relief surface deformation. Taking an advantage of a generalized norm approach in the formulation, we have applied the present method to three-dimensional volume morphing. A preliminary result suggests that the method applies as long as the shape involved is sufficiently smooth. A possibility is sought for extension to general shapes.

1. Introduction

Digital image warping defines the spatial relationship between points in images by some geometric transformation. The transformation is based either on field warping where features of relevant deformations in images are specified or mesh warping where deformation of meshes are specified as in free form design method (Wolberg[1]). Image warping plays an important role in a wide range of applications including remote sensing, medical imaging, computer graphics as well as in computer vision fields[1]. Although we address to an image morphing application in this paper, the fundamental algorithms used in digital image warping are so closely related, we will review the subject from a general point of view first, highlighting the detailed review on morphing scheme in Section 2.

In remote sensing, for example, multi-image sets of Landsat require elaborate corrections of images to account for different sensor distortion properties used if accurate image registration or exact matching of all corresponding points in image sets is needed.

Computer graphics abounds in important applications: Using the thin-plate spline transformation, Bookstein's extensive morphometric studies[2] of biological organs or of externally observable phenytoin-affected human facial features have been remarkably successful in providing plausible explanations respectively for ecological changes of the past or invisible neuroteratogens which must have taken place during pregnancy perhaps deep within the central structures in the frontal lobe of a fetus due to drug infection. Yan and Tokuda[3] have applied Bookstein's method to the problem of automatic analysis and recognition of biomedical organs for possible use in computer-aided diagnosis and other medical applications. They are able to show that a considerable variability of individual organs can be accounted for by the transformation, marking a first step in fulfilling the purpose. For implementation of automatic recognition of such organs, much still remains to be explored so that automatic extraction of feature points of both model and destination

† Computer Science Department, Faculty of Engineering, Utsunomiya University
†† Faculty of International Studies, Utsunomiya University

objects becomes possible. At present, extraction of feature points are done interactively.

Other important computer graphics applications include geometric model generation in CAD or CAGD (Farin[4]) or free-form surface design applications ranging from art to engineering designs (Welch & Witkin[5], Kallay[6], Cheng & Barsky[7] and Wyvill & McRobie[8]) with both problems being closely related. Generating smooth interpolated curves and surfaces subject to various constraints imposed with a minimum computational cost constitutes the important requirements of image warping in these applications. Image morphing to which we directly address in this paper, is another emerging field of interest in computer graphics attracting keen interest recently particularly among CG specialists, TV and other commercial audiences. A review on the subject is given in the following section.

In computer vision, image warping has posed a different, quite demanding requirement of producing smooth data interpolations and data approximations, the latter requiring an introduction of discontinuities within the same image; Grimson[9] and Terzopoulos[10] have tried to overcome the difficulty by introducing regularization schemes into a solution method of variational principles to make the ill-posed inverse visual problems well-posed because 3-D images need to be reconstructed from the inadequate, sparse 2-D images. In addition to usual spline-type quadratic variations having smoothing constraints, the first order variations of membrane type are introduced as a minimizing functional, the latter allowing a derivative discontinuity namely of C^0 surface.

In Section 2, we will specialize to, and review computational methods used in, morphing techniques. In Section 3, we formulate the global spline-type transformation under the paradigm of generalized norm minimization based on M-th Sobolev semi-norm in N-dimensional space (Wolberg[1]). The formulation includes a minimum bending energy paradigm of Bookstein[2] and Yan & Tokuda[3] as a special case. The method is then applied to an image metamorphosis problem of two-dimensions in Section 4.1 with computed results being compared with existing methods. In Section 4.2, the analysis of this paper is applied to 2.5D problem of a relief surface problem where the two-dimensional analysis of Section 3 is apparently valid. Taking an advantage of the generalized formulation of the present method, an extension to fully 3D applications is attempted in Section 4.3, giving a preliminary result to a fully three-dimensional application, the results being tentative.

We show that among the several methods used in metamorphosis, the globally valid spline-type transformation we use here not only best meet the fundamental requirements of morphing, the method is nevertheless general enough to apply to most of the other applications we have discussed in the preceding paragraphs.

2. Morphing Techniques

Due to its important applications in animation with a sequence of inbetween images changing from some source image to another destination image over time, the image morphing technique calls for the following four requirements.

(a) Efficient computational complexity,
(b) ease of specifying feature points or lines for characterizing images in both source and destination images,
(c) accurate fitting of specified interpolating points and
(d) generating smoothed curves or surfaces having at least C^1 continuity or higher.

The first problem of computational complexity is perhaps the more crucial to morphing applications because of its possible use in animation requiring a long sequence of image frames. The other three requirements have more or less a more general need in other applications of image distortions including image recognition. As classified by Wolberg[1], field warping is oriented to feature-based morphing while mesh warping to free form design scheme based on B-spline surfaces or Bezier patches.

Beier and Neely[11] seem to be the first to introduce a first practical computational scheme into morphing technology based on field warping; it is based on the feature-based image metamorphosis scheme whereby feature lines drawn in source and destination images are used in image warping. For example, the distances defined between any intermediate pixel point to the pairs of feature lines drawn in source images are used by somewhat empirical formula to locate the warped position of the pixel in the destination image by taking weighted averages of all the lines drawn. Unlike the present method where feature points are selected along image objects (see Section 3 for a detailed description of this point), feature lines

are selected instead in their method. In fact, their choice seems critical in producing good visual effects. Optimal choice of feature lines often gives remarkably expressive animated effects. Unlike more rational global coordinate transformation of minimum bending energy or spline-based transformation schemes to be discussed below, the method often suffers from two serious drawbacks; firstly from isolated ghost images produced particularly for points near the line intersections, and more seriously from slow running performance if the number of feature lines increases.

A typical mesh warping scheme is applied by Nishita et al.[12] to the morphing problem where free form deformation method and the Bezier clipping scheme are combined. To ensure C^1 continuity not only along boundaries of distorted images but everywhere within the image, mesh points overlaid on images are used as control points of bicubic Bezier patches. Because mesh points, image contours and feature points in particular seldom align, we have to depend heavily on linear interpolations of intermediate mesh points for most of the image warping implementation. Contour lines of both source and destination images are computed by scanline algorithm of inverse mapping. The drawbacks of the scheme come partly from the inability of specifying the more direct feature points of images and also time consuming scanline inverse mapping for locating exact pixel points in the source and destination images which are needed for texture information for example. Because of the fast operations involved in Bezier clipping and scanline algorithm, the computational time is surprising fast as we discuss in Section 5 in details.

Lee et al.[13], on the other hand, formulate the 2-D morphing problem as a variational problem along the computational scheme of Terzopoulos[10] used in computer vision applications where in addition to the quadratic variation of bending energy functional, functionals representing the zeroth order variations of the spring energy and the glue energy are minimized simultaneously. This ensures a C^1 continuous deformed surface. The glue energy has an effect of localizing the distortion effected. See Section 4 how our scheme is capable of localizing the deformation. The formulated discretized problem is solved by an efficient multigrid scheme which, unlike the more popular SOR (successive overrelaxation) scheme of solution, very effectively handles high frequency as well as low frequency errors simultaneously by adaptively changing the grid size during the solution process resulting in linear order calculation in unknowns, namely, for a $G = W \times H$ regular grid size where W and H amounts to 512×512 pixels in general, the algorithm is known to converge to the first order complexity of O(G).

Three-dimensional morphings have been attempted recently, using the Fourier transform by Hughes[14] and the wavelet transform by He et al.[15] where three-dimensional volume morphing between topologically different objects are tried. We will not go into details on the subject and merely present a preliminary result on 3D volume transformations within the framework of a generalized norm minimizing paradigm in Section 3 below.

3. Formulating Deformable Spatial Transformations

Following Yan & Tokuda[3], consider mapping a set of n points $\mathbf{p}_i$ in the N-dimensional model space to another set of n points $\mathbf{p}'_i$ in the N-dimensional warped destination space; the n points are called landmarks by Bookstein[2]. In image analysis field, the n points are more aptly called feature points of the images characteristic of the shape of the object to map. Feature points can be associated with corners, inflection points, cusps located between convex and concave curves of digital curves as discussed in 16), for example. We emphasize that the selection of feature points may be far more effective than that of feature lines of Beier & Neely[11] and that they can be in either two- or three-dimensions. They are in fact extremely sparse as compared with the total number of pixel points $G = W \times H$ that an accurate and robust scheme of interpolation or approximation is called for. We generalize below the thin-plate spline theory of Bookstein[2] and Yan & Tokuda[3] based on minimization of second order derivatives of displacement squared to a more general M-th order derivatives of displacement squared in N-dimensional space. The mapping function must satisfy

$$\mathbf{f}(\mathbf{p}_i) = \mathbf{p}'_i \quad \text{for} \quad i = 1, 2, \ldots, n. \tag{1}$$

Here, $\mathbf{f}$ is a N-vector function so that $\mathbf{f} = (f_1, f_2, ..., f_N)$. Similarly since $\mathbf{p}_i$ and $\mathbf{p}'_i$ are points in N-dimensional space, they stand for N-vector constants. To obtain a unique

mapping function $\mathbf{f}$ from source to destination space, consider minimizing the following functional $I(\mathbf{f})$ as,

$$I(\mathbf{f}) = \int_{R^N} g_N^M(\mathbf{f}) dx_1 \dots dx_N \qquad (2)$$

where the minimizing goal function $g_N^M(\mathbf{f})$ involving a hierarchy of successively higher derivatives, upto M-th order, of displacement squared is defined as (Ienaga[19] and Wolberg[1]),

$$g_N^M(\mathbf{f}) = \sum_{i+j+\dots+k=M} \binom{M}{i} \times \left(\frac{\partial^M \mathbf{f}}{\partial x_1^i \partial x_2^j \dots \partial x_N^k} \right)^2 . \qquad (3)$$

A class of minimizing functions to Eq. (2) can be obtained in terms of fundamental solutions to a biharmonic equation $\Delta^2 \mathbf{f} = 0$ with $\Delta = \sum_{i=1}^N \partial^2/\partial x_i^2$ for $M = 2$ and to a tri-harmonic equation $\Delta^3 \mathbf{f} = 0$ for $M = 3$ (see Ienaga[19]).

In terms of $r = (\sum_{i=1}^N x_i^2)^{1/2}$, the fundamental solution $U_N^M(r)$ can be given as

$$U_N^M(r) = \begin{cases} C \times \dfrac{1}{r^{N-2M}} \\ (\text{if } N - 2M > 0 \text{ or} \\ \text{negative odd integers}) \\ \\ C \times \dfrac{\log(r)}{r^{N-2M}} \\ (\text{for } N - 2M = 0, -2, \dots) \end{cases} \qquad (4)$$

where

$$C = \frac{\Gamma(N/2)}{2^M (M-1)! \pi^{M/2} \prod_{k=1}^M (2k - N)} .$$

In terms of $r_{ij} = |\mathbf{p}_i - \mathbf{p}_j|$ which denotes the ordinary Euclidean distance between points $\mathbf{p}_i$ and $\mathbf{p}_j$, we can construct the mapping functions $\mathbf{f}$ as follows (see Yan & Tokuda[3] or Bookstein[2]).

$$K = \begin{bmatrix} 0 & \cdots & U_N^M(r_{1n}) \\ U_N^M(r_{21}) & \cdots & U_N^M(r_{2n}) \\ \vdots & \vdots & \vdots \\ U_N^M(r_{n1}) & \cdots & 0 \end{bmatrix}, \qquad (5)$$

$$P = \begin{bmatrix} 1 & \mathbf{p}_1 \\ 1 & \mathbf{p}_2 \\ \vdots & \vdots \\ 1 & \mathbf{p}_n \end{bmatrix}, \qquad (6)$$

$$L = \begin{bmatrix} K & P \\ P^T & 0 \end{bmatrix}, \qquad (7)$$

$$Y = \begin{bmatrix} \mathbf{p}_1' & \cdots & \mathbf{p}_n' & 0 & \cdots & 0 \end{bmatrix}^T . \qquad (8)$$

We can get a spatial mapping satisfying $\mathbf{f}(\mathbf{p}_i) = \mathbf{p}_i'$ only if the determinant $L \neq 0$. Then we have

$$L^{-1} Y = \begin{bmatrix} \mathbf{w}_1 \\ \cdots \\ \mathbf{w}_n \\ \mathbf{a}_0 \\ \cdots \\ \mathbf{a}_N \end{bmatrix} . \qquad (9)$$

For any $\mathbf{x} = (x_1, x_2, \dots, x_N)$ in source space, the vector mapping function $\mathbf{f}$ is then given as,

$$\mathbf{f}(\mathbf{x}) = \mathbf{a}_0 + (\mathbf{a}_1 \cdots \mathbf{a}_N)\mathbf{x}^T + \sum_{i=1}^n \mathbf{w}_i U_N^M (|\mathbf{p}_i - \mathbf{x}|) . \qquad (10)$$

This is a global spatial mapping minimizing the entire integral of goal functions of Eq. (2) over the entire space of the M^{th} Sobolev seminorm (Wolberg[1]). The mapping is now valid over the entire domain including interior as well as exterior, outer boundary points of the domain.

The physical validity of minimization of the goal function g_2^2, a special case of $M = 2$, $N = 2$ in Eq. (10), has been well established as a smoothing constraint of curves in two-dimensions or surfaces formed of thin sheets in three-dimensions because it approximates the bending energy along the entire thin-sheet (Bookstein[2] and Yan & Tokuda[3]). We need cautions in extending the thin-plate spline theory of two-dimensions to three-dimensions or higher, because whether or not minimization of g_3^2 is capable of playing a similar role of smoothing constraint of comparable two-dimensional g_2^2 function is not much clear. The tensorial nature of stresses will not guarantee the validity of g_3^2 function as bending energy in 3D. In fact, we know from 2) and 3) that the fundamental solution U_3^2 to g_3^2 function apparently fails to give a C^1 continuity at all of the interpolated points of feature points. To ensure a C^1 continuity, U_3^3 can be used and a preliminary result of transformation is presented in Section 4.3 where possible problem areas in the present approach will be contrasted with the more recent methods of interpolation using reproducing kernels of Sobolev spaces[17),18]. Unlike the Fourier transform or wavelet transform methods suggested by Hughes[14] and He et al.[15] respectively, the analytical scheme of this paper may not be expected to be applicable to objects of different topology as it is.

4. Applications to Image Morphing

4.1 Two-Dimensional Applications

We present below several morphing applications using the thin-plate global deformation technique we described in Section 3. Note that unlike feature lines of Beier & Neely[11], we can select feature points along image profiles subjected to warping. This adds considerable flexibility to the present method as we show below. Morphing problems can easily be implemented by a sequence of time series between the source and the target images. Given two images of I_0 of source image and I_1 of destination image, the image morphing problem is to find a sequence of inbetween images $I(t)$, for $0 \leqq t \leqq 1$, such that $I(0) = I_0$ and $I(1) = I_1$. We assume that time t varies from 0 to 1 so that the source image I_0 continuously changes to the destination image I_1. The inbetween images of $I(t)$ are defined by creating a new set of feature points by linearly interpolating the feature points from their positions on I_0 to the positions on I_1. For each pixel point $p(t)$ on an inbetween image $I(t)$, we can find its corresponding mapping position $p(0)$ on I_0 and $p(1)$ on I_1 using the matrix inversion (9) as well as the mapping function (10). The colors of pixel $p(t)$ is obtained by cross-dissolving of colors of $p(0)$ to colors of $p(1)$.

To show the effectiveness of our method in morphing application, we have chosen a rather severe test of deforming a geometric model of a letter 'F' to letter 'T'. We align all the edges of the letters 'F' and 'T' along 22×22 grid lines as shown in **Fig. 1** a and Fig. 1 b. In fact, the letter 'T' of Fig. 1 b is obtained by specifying 80 intersections of grid lines with the exterior straight edges of the letters 'F' and 'T' as feature points but all other points are left free with no other constraints imposed during warping. The reconstructed image of distorted letter 'T' of Fig. 1 b is shown together with the warped grid lines demonstrating the degree of distortion needed for this image morphing. Computations involving the matrix inversions of Eq. (9) are first carried out at every feature points specified and the closed form solution in Eq. (10) are used to compute the geometric distortion of grid lines. Despite such a severe straining distortion exerted, it is surprising that the outer edges of letter T remain straight although free grid lines are severely distorted near regions of severe straining motions such as intruding cavity-like region near the middle web section of F. The region looks like a cavity because grid lines within the letter portion is drawn in white color.

Now we demonstrate below how we can introduce and specify, additional feature points for the purpose of constraining the extent of distortion. We have added constraining feature points in the following manner;

(a) three rows of outermost exterior grid points comprising the square box containing the letter F and T which amounts to 209 constraining feature points (20 points along upper horizontal line being excluded because both F and T are not subjected to any considerable warping in the region),

(b) 20 interior grid points of middle web region of F and

(c) 7 grid points at the foot of F letter.

209 points in (a) are introduced to localize the distortion within the 22×22 box. 20 points of (b) are added to avoid possible cavity-like intruding grid lines of Fig. 1 b. The transition of inbetweens from letter F of Fig. 1 a at $t = 0$ to final letter T is shown in Figs. 1 c, d, e and f at $t = 0.25$, 0.5, 0.75 and 1.0 respectively. Unlike Lee et al.[13] where the glue energy is used to effect localization, the present solution use feature points of (a) above as fixed points of the transformation along the small enough box area of letter F so that no influences are exerted outside of the inner square region. See Yan & Tokuda[3] for further discussions on other aspect of localizing effects of the present method where the effect of distortion dies out like $1/r$ away from the feature point. This localization effect is extremely useful very often in morphing and animation applications because often only local adjustments are needed. It is instructive to see the process of the distortion as time elapses by observing the originally square grids keeps deforming while in less strained regions they remain square. Our approach should be contrasted with that of Nishita et al.[12] where mesh points and lines are directly subjected to warping, rather than the specified feature points of our scheme.

We now turn to image problems. The first example of **Figs. 2** a, b and c presents morphing from the face of a caracal to a puma using 75 feature points shown by cross symbols on the images. Figures 2 a and b are respectively the source image of caracal and the target image of puma while Fig. 2 c shows an intermediate

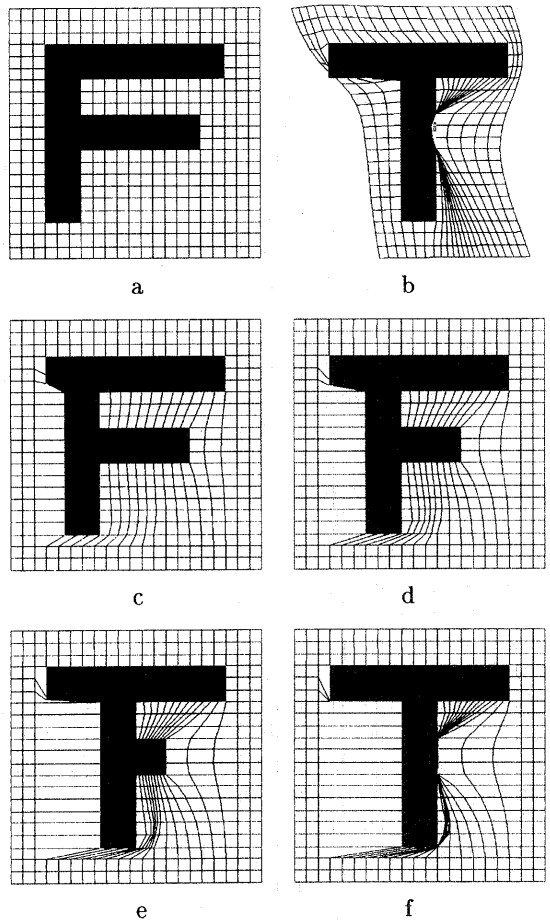

Fig. 1 From left to right, top to bottom. a: Original image of the letter F, b: Distorted image of letter T from F, c: Local distorted image of T from F at $t = 0.25$, d: at $t = 0.5$, e: at $t = 0.75$, f: at $t = 1$.

image at $t = 0.5$ from the morphing sequence of images. The picture size is 400×400.

The second example is taken from Beier & Neely[11] where 56 feature points selected are marked by crosses. The picture size chosen is 568×432 pixels. **Figures 3** a, b are the original source and target images of 11) while Fig. 3 c is an intermediate image as given by Beier & Neely where time t is not given. The intermediate image given by our method is shown in Fig. 3 d at $t = 0.5$.

Compared with the methods of Lee et al.[13] or Nishita et al.[12] where computations must be carried out over all pixel points, our scheme has two distinct advantages; firstly the core computations of the present method involving a matrix inversion extends only to the far sparse, feature points (see Eq. (9)). Furthermore, the closed form of solution of the present method allows us to reconstruct the images more efficiently by a block region basis where within each of the block regions, we can apply more efficient linear interpolations rather than going through tedious summation calculations of Eq. (10) over the entire feature points. Time complexity analysis together with the quality of the image will be presented in Section 5 in details. We show that a significant reduction in time is obtained for 16×16 block size without any visual deterioration in picture quality. This is a distinct advantage in animation applications because considerable saving can be obtained where a long sequence of frames are always needed.

4.2 Two and Half-Dimensional Applications

A straightforward extension of 2-D approach to 3-D can be attempted to a 2.5-D application of **Fig. 4** a where Japanese Noh masks are deformed from a two-dimensional sheet. Since the deformation specified is essentially always vertical with a three-dimensional relief surface being constructed from a two-dimensional sheet, the warping is strictly two-dimensional in nature, hence the goal function g_2^2 of Eq. (3) is used for minimization. The picture is treated as a plan in a three-dimensional space thus warping the two-dimensional image plan to form a three-dimensional elevated surface. The texture of the mask can be automatically mapped on to the surface. We have used a total of 164 landmarks in the transformation where 148 points are used for expressing featuring elevated points within the mask while the remaining 16 points are used in expressing the support of a relief plane around the mask. This support plane is necessary to ensure the non-zero determinant of matrix L of Eq. (7). Figure 4 b is the rendered result after the transformation with the texture mapping on to the surface.

4.3 Preliminary Results in Three-Dimensional Applications

As a preliminary experiment to fully three-dimensional application, we have selected a three-dimensional CT head volume data of **Fig. 5** a with an ear portion eliminated, because we know that the ear portion has unusually a complicated configuration of very rapid variations with a number of singular points demanding an entirely new method of analysis[20]. We have used the goal function of g_3^3 of Eq. (3) rather than the function g_3^2 which is intention-

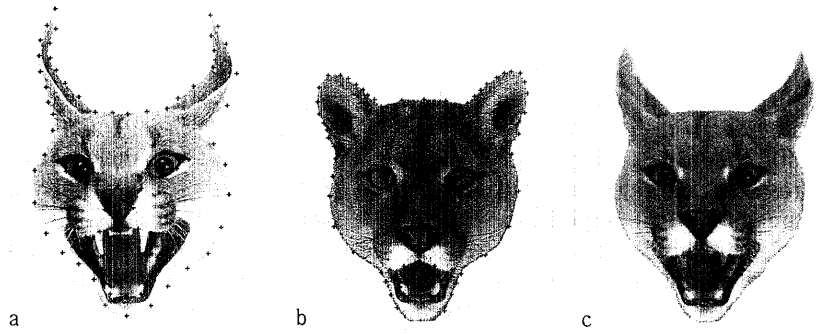

a b c

Fig. 2 From left to right. a: Source image of a caracal with landmarks, b: Destination image of a puma with landmarks, c: Intermediate image of our method at $t = 0.5$.

a b

c d

Fig. 3 From left to right, top to bottom. a: Source image of a man with landmarks, b: Destination image of a woman with landmarks, c: Intermediate image of Beier and Neely, d: Intermediate image by our method at $t = 0.5$.

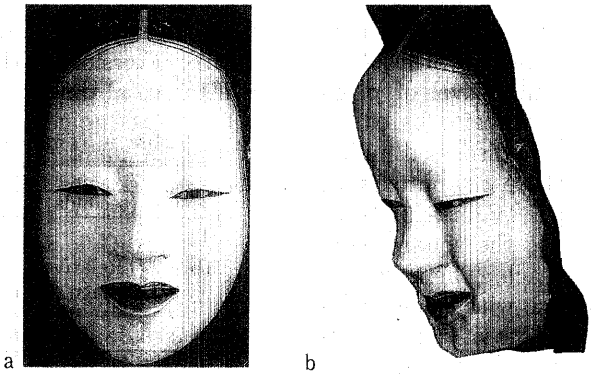

a b

Fig. 4 From left to right. a: Image of a Japanese Noh mask, b: 3D rendering with texture mapping.

ally avoided here to ensure C^1 continuity everywhere (see our discussions in Section 3 for details). A cubic variation rather than a quadratic variation in the calculus of variations is used. But a higher value of M chosen will inevitably increase the instability due to high frequency part of profiles resulting in undesirable ripplings in the warped image. In the experiments, we have used a simple threshold in tracing the surface of the head in volume data. A sphere and the rendered CT model are used as the source and the target images. The corresponding feature points of the target and source images are located at the intersections of radial rays emanating from the center of sphere with the CT head and the sphere. Fewer points are chosen near the skull as compared with the facial part.

Figures 5 b and c are the rendering results of the processing which used 418 and 1170 feature points respectively. So we see that the present approach is applicable in 3D if the variations of shapes are reasonably small. Undoubtedly we do need a more stable method of interpolations for general purpose shapes. This may be achieved by extending the works of 17) and 18), the latter needing an extension to 2 and 3D. We would like to examine the extension in the future. It seems likely that the present transformation of $M = 3$ is applicable as long as the variations are fairly smooth.

5. Discussions

It is instructive to examine the computational complexity of the morphing methods we have discussed in this paper.

Examining Eqs. (9) and (10) of Section 3, the computational complexity of our method is of $O(n^3)$ for Eq. (9) and O (nG) for Eq. (10), where G is the total number of pixels in the image, n is the number of feature points specified. This is so because the contributions from each feature point must be summed up in Eq. (10). Unless the color level or grey level of pixels change very rapidly, the block region based image reconstruction scheme we discussed in Section 4.1 is quite powerful where we approximate the image color or grey level by linear interpolations. Suppose we choose the square block region having $b \times b$ pixels each. The number b can be chosen in accordance with image quality required. The four points at the corners of each block region in both source and destination images must be computed by Eq. (10) but at the remaining $b \times b - 4$ pixels out of the entire b^2 pixels, the image is reconstructed by simpler linear interpolation requiring the complexity of b to determine the equivalent pixel position in source and target images per pixel so the computational complexity of this portion can be shown to be reduced from O (nG) to O $(G(b + n/b^2))$. An optimal value of b for minimizing the computational complexity actually depends on n and also we must be cautious to see that the quality of the image color information is not lost. We have made extensive experiments on the model morphing of Beier & Neely[11] as given in Figs. 3 a through c. For the 568 × 432 size picture of Beier & Neely[11], we have obtained the following time measurements. Our main work was implemented on the AVS system of a Kubota Vistra/B workstation, but to facilitate comparisons of computing time with other methods, we have also used a SGI indigo2 (R4000) such as the times of **Table 1** below.

As to color quality of the picture, we took differences in RGB values at each pixel for b =1, 2, 4, 8, 16 obtaining the following results. The values in **Table 2** are for R values which average to 191.17 out of possible 256 levels.

As long as we see with our eyes, we can not recognize any visual differences in the images at all between images of $b = 1$ and $b = 16$ where 99.3% of all pixels have differences of level 5 or less for the average of 191 R levels. We see that the quality of images obtained at $b = 8$ and $b = 16$ seems sufficient to give a best possible choice from both the time complexity and the image quality point of view. The quality of the images is equivalent to those obtained directly from Eq. (10) pixel by pixel basis. An entirely similar situation holds for experiments of Fig. 2. The computational time in reconstructing the images of 400 × 400 color pictures with 75 feature points is less than 1 second for matrix inversion of the present scheme of (9) and the total time for generating an inbetween

Table 1 Time measurements for size b.

b	1	2	4	8	16
time (seconds)	86	25	10	6	5

Table 2 Relative number of pixels having given range differences in R values.

	diff=0	diff≤1	diff≤5
$b = 4$	95.97%	99.93%	99.99%
$b = 8$	91.42%	99.06%	99.95%
$b = 16$	82.97%	94.87%	99.32%

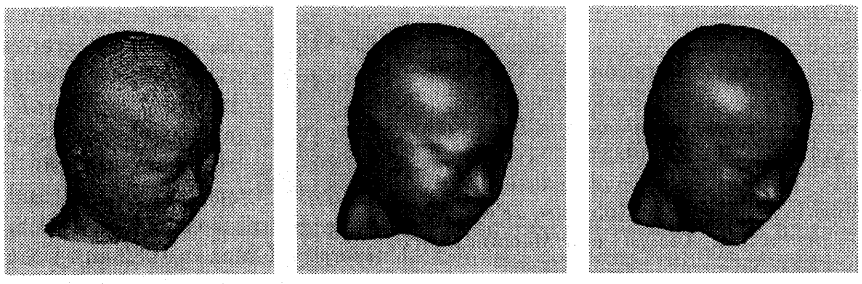

a b c

Fig. 5 From left to right. a: Surface rendering of CT head volume data, b: 3D rendering result with 418 landmarks, c: 3D rendering result with 1170 landmarks.

image is about 77, 22, 8, 5 and 4 seconds when block region size of 1, 2, 4, 8, and 16 are used respectively. For the morphing of similar picture size of 500 × 400, Nishita et al.[12] took 22 seconds with Indigo2 R3000 which is perhaps comparable to 10 seconds for our R4000 machine. Lee et al.[13] report the generating time of a 449 × 423 size inbetween image of 23.6 seconds with R4000 indigo2. As far as we know, our time seems the best published times in morphing literature.

The computational complexity of Beier and Neely's method[11] can be estimated to about (nGW_1), where n is the number of the feature lines and W_1 is amount of computation required for one pair of feature line. The time complexity of Lee et al.'s[13] is of O $((7/2)\nu W_2(G))$, here ν is the number of relaxation required on each of a grid, W_2 is the amount of computation required for one relaxation on the finest grid, which is apparently proportional to the G of total pixels. However, in their method all pixel points constitute unknowns so that the entire pixel points must fully be convergent to a tolerable level before we can use the solution as the image.

In all of our image morphing experiments, we found that around one hundred landmarks or feature points are adequate to get a satisfied shape interpolation. The computational speed of our method is fast enough for an interactive environment. In all likelihood, we need a more stable computational scheme for 3D applications along the lines of Duchon[17] and Watanabe[18].

Acknowledgments We are most grateful to the referees for their most valuable comments to the first draft of this paper which led to a substantially improved presentation of the paper. We also extend our sincere appreciation to the members of our Research Group for their helpful comments and encouragement. We have received financial support for the present research from Toshiba Medical Engineering Company. The first author has been supported partly by a research-in-aid grant from Ashigin International Foundation of Ashikaga Bank for the last three years. We are grateful to all of them.

References

1) Wolberg, G.: *Digital Image Warping*, IEEE Computer Press, LA, Calif. (1990).
2) Bookstein, F.L.: Principal Warps: Thin-Plate Splines and Decomposition of Deformation. *IEEE Transactions on Pattern Analysis and Machine Intelligence*, Vol.11, No.6, pp.567–585 (1989).
3) Yan, R.H. and Tokuda, N.: Analysis and Recognition of Medical Images: 1, Elastic Deformation Transformation, *Communicating with Virtual Worlds*, Thalmann N.M. and Thalmann D. eds., Springer-Verlag, pp.580–593 (1993).
4) Farin, G.: *Curves and Surfaces for Computer Aided Geometric Design*, Academic Press, (1990).
5) Welch. W. and Witkin, A.: Variational Surface Modeling. *Computer Graphics (Proc. SIGGRAPH)*, Vol.26, No.2, pp.157–166 (1992).
6) Kallay, M.: Constrained Optimization in Surface Design. *Modeling in Computer Graphics*, Falcidieno B. and Kunii T.L. eds., Springer-Verlag, pp.85–93 (1993).
7) Cheng, F.H. and Barsky, B.A.: Interproximation Using Cubic B-Spline Curves. *Modeling in Computer Graphics*, Falcidieno B. and Kunii, T.L. eds., Springer-Verlag, pp.359–374 (1993).
8) Wyvill, G. and McRobie, D.: Local and Global Control of Cao En Surfaces, *Communicating with Virtual Worlds*, Thalmann M.N. and

Thalmann D. eds., Springer-Verlag, pp.216–227 (1993).
9) Grimson,W.: An Implementation of a Computational Theory of Visual Surface Interpolation, *Computer Vision, Graphics, and Image Processing* Vol.22, pp.39–69 (1983).
10) Terzopoulos, D.: Regularization of Inverse Visual Problems Involving Discontinuities, *IEEE Transaction on Pattern Analysis and Machine Intelligence* Vol.8, No.4, pp.413–424 (1986).
11) Beier, T. and Neely, S.: Feature-Based Image Metamorphosis, *Computer Graphics (Proc. SIGGRAPH)*, Vol.26, No.2, pp.35–42 (1992).
12) Nishita, T., Fujii, T. and Nakamae, E.: Metamorphosis Using Bezier Clipping, *Proceeding of the First Pacific Conference on Computer Graphics and Applications*, pp.162–173 (1993).
13) Lee, S.Y., Chwa, K.Y., Hahn, J. and Shin, S.Y.: Image Morphing Using Deformable Surfaces, *Proceeding of Computer Animation '94*, IEEE Computer Society Press, pp.31–39 (1994).
14) Hughes,E.S.: Scheduled Fourier Volume Morphing,*Computer Graphics*, Vol.26, No.2, pp.43–46 (1992).
15) He, T., Wang. S. and Kaufman, A.: Wavelet-Based Volume Morphing. *Proceeding of IEEE Visualization'94*, Washington, D.C., Oct. (1994).
16) Pikaz, A. and Dinstein, I. Using Simple Decomposition For Smoothing and Feature Point Detection of Noisy Digital Curves, *IEEE Transaction on Pattern Recognition and Machine Intelligence*, Vol.16, No.6, pp.808–813 (1994).
17) Duchon, J.: Splines Minimizing Rotation-Invariant Semi-Norms in Sobolef Spaces, *Lecture Notes in Math.* Vol.571, Springer-Verlag, pp.85–100 (1977).
18) Watanabe, K.: An Interpolation Method Using a Reproducing Kernel of Sobolev Space $H_o^s(\Omega)$, *Journal of Information Processing Society of Japan*, Vol.35, No.10, pp.1978–1887 (1994).
19) Ienaga, Y.: *Handbook of Mathematics*, Third edition, Mathematical Society of Japan ed., Iwanami Publishing Company. (in Japanese) (1988).
20) Shinagawa, Y. and Kunii, T.L.: The Homotopy Model: A Generalized Model For Smooth Surface Generation From Cross Sectional Data, *The Visual Computer*, Vol.7, pp.72–86, (1991).

(Received November 24, 1994)
(Accepted October 5, 1995)

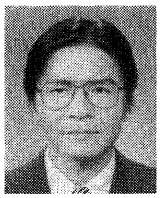

Ronghua Yan is currently a doctoral graduate student in Computer Science Department, Faculty of Engineering at Utsunomiya University. His research interests include computer graphics and image processing. He received B.S. and M.S. from Fudan University, China in 1982 and Utsunomiya University, Japan in 1993 respectively. He had joined Shanghai Institute of Computer Technology as a research assistant during 1982 to 1989 on computer network and expert system. He is a student member of IPS, Japan.

Naoyuki Tokuda is a Professor in Computer Science Department, Faculty of Engineering at Utsunomiya University. His present interest includes computer graphics, image analysis and recognition, intelligent tutoring systems in AI, sorting analysis and informatics education. Tokuda has received his B.S., M.S. and Ph.D. degrees from Yokohama National University in 1959, Stanford University in 1962 and University of Michigan in 1966 all in mechanical engineering respectively and D.Sc. from University of Tokyo in 1975. He has been a visiting fellow at DAMTP, University of Cambridge during 1969–1971 and a senior scientist at Mathematics Department of Southampton University during 1971–1972. He is a member of IPSJ, IEEE, Computer Graphics Society, Society for Science on Form of Japan, Physical Society of Japan and Japan Society of Fluid Mechanics. He can be reached at e-mail: tokuda@cc.utsunomiya-u.ac.jp

Juichi Miyamichi received the B.S., M.S. and Ph.D. degrees in Electrical Engineering from Tokyo Institute of Technology, Tokyo, Japan in 1971, 1973, 1976, respectively. From 1976 to 1979, he was a research assistant at Tokyo University of Agriculture and Technology. After being an associate professor from 1979 to 1991, he has been a Professor at the Department of Information Science, Faculty of Engineering, Utsunomiya University, Utsunomiya, Japan. His research interests include control theory, system theory and digital image processing. He is a member of the Institute of Electrical Engineering of Japan, the Society of Instrument and Control Engineers in Japan and Japanese Society for Artificial Intelligence.

Yongmao Ni received his B.S. from Utsunomiya University in 1985, and his M.S. and Ph.D. degrees from Tokyo Institute of Technology in 1987 and 1990. He is working now in Faculty of International Studies at Utsunomiya University. His present interest includes computer graphics, communication protocol validation and data compression. He is a member of IEICE, Japan. He can be reached at e-mail: niy@utsunomiya-u.ac.jp